



# OPEN Development and evaluation of Chia seed-based nanofibers and nanoemulsions for *Bacillus coagulans* Encapsulation

Shirin Rashnoei<sup>1</sup>, Mozghan Shahamirian<sup>2</sup>✉, Sedigheh Yazdanpanah<sup>3</sup> & Elham Ansarifard<sup>4</sup>

This study explores the encapsulation efficiency of composite nanofibers and nanoemulsions derived from chia seed mucilage (*Salvia hispanica* L.), a natural hydrocolloid with notable bioactive properties. Nanofibers, known for their high surface area and stability, and nanoemulsions, recognized for their enhanced bioavailability, were utilized to encapsulate *Bacillus coagulans*. Chia mucilage demonstrated a DPPH radical scavenging activity of 67.88% at 350 µg/mL and moderate antimicrobial effects, with inhibition zones of 9 mm and 6 mm against *Staphylococcus aureus* and *Escherichia coli*, respectively. Nanofibers prepared with 2–3% mucilage showed uniform morphology (diameters: 12.36–26.24 µm) and significantly higher encapsulation efficiency ( $93.90 \pm 2.1$ ) ( $p < 0.05$ ) than nanoemulsions ( $88.33 \pm 2$ ). FTIR analysis confirmed the successful encapsulation of *Bacillus coagulans*, with characteristic peaks in the ranges of 1500–1600 cm<sup>-1</sup>, 2800–3000 cm<sup>-1</sup>, and 3200–3500 cm<sup>-1</sup>. These findings suggest that chia seed mucilage-based nanofibers offer a stable and efficient platform for probiotic delivery, with promising applications in functional foods, pharmaceuticals, and cosmetics.

**Keywords** *Bacillus coagulans*, Chia seed, Nanofibers, Nanoemulsion, Electrospun

## Abbreviations

ATCC	American Type Culture Collection
CFU	Colony Forming Units
DDW	Double-Distilled Water
DLS	Dynamic Light Scattering
DPPH	2,2-Diphenyl-1-picrylhydrazyl
FTIR	Fourier Transform Infrared Spectroscopy
IC50	Half Maximal Inhibitory Concentration
NYSM	Nutrient Yeast Extract Salt Medium
PVA	Polyvinyl Alcohol
RSA	Radical Scavenging Activity
SEM	Scanning Electron Microscopy
SOD	Superoxide Dismutase
ZOI	Zone of Inhibition

Nanotechnology involves the manipulation of matter at dimensions ranging from 1 to 100 nm, enabling the development of new applications through unique phenomena<sup>1,2</sup>. Among the various nanostructures, nanofibers are particularly suitable due to their ease of preparation from a wide range of natural and synthetic polymers. Their production is highly controllable, allowing for the manipulation and alteration of functional properties during the manufacturing process. Nanofibers can be employed as carrier systems for delivering antimicrobial agents, drugs, dyes, flavors, antioxidants, and other functional compounds<sup>3,4</sup>. Nanocomposites reinforced with nanofibers are a prominent example of advanced nanomaterials. Nanofibers can be produced by various

<sup>1</sup>Department of Food Science and Technology, Sarvestan Branch, Islamic Azad University, Sarvestan, Iran.

<sup>2</sup>Department of Chemistry, Faculty of Science, Sarvestan Branch, Islamic Azad University, 73451-173 Sarvestan, Iran. <sup>3</sup>Department of Food Science and Technology, Kazerun Branch, Islamic Azad University, Kazerun, Iran.

<sup>4</sup>Department of Public Health, School of Health, Birjand University of Medical Science, Birjand, Iran. ✉email: mozhgan.shahamirian@iau.ac.ir

methods, with electrospinning being one of the most common techniques<sup>5,6</sup>. In this method, a high voltage creates a potential difference between the needle tip containing the polymer solution and the collection plate. This causes a continuous jet of polymer to form, with the entangled polymer chains preventing the fiber strand from breaking. The electrical charge draws the fibers towards the collection plate, facilitating fiber formation<sup>7–9</sup>.

Various polymers, including polyvinyl alcohol (PVA), are widely utilized in electrospinning due to their versatile properties. PVA, as a water-soluble, biodegradable, and cost-effective polymer, has been extensively used in creating polymer nanocomposites. Its polar nature and ability to form strong intermolecular bonds make it a suitable candidate for enhancing the stability and structural integrity of nanofibers<sup>10–12</sup>.

In addition to synthetic polymers like PVA, natural biopolymers are gaining attention due to their biocompatibility and functional properties. Chia (*Salvia hispanica* L.) mucilage, a polysaccharide-rich hydrocolloid, has emerged as a promising material for nanofiber production. Its high viscosity, adhesive properties, and film-forming ability ensure good flowability and stability during electrospinning, making it particularly suitable for biomedical and food applications<sup>13–15</sup>.

Phosphocasein peptides, derived from casein hydrolysis, also contribute significantly to nanofiber fabrication. These peptides, due to their phosphorylated groups, enhance hydrogen bonding and ionic interactions within the polymer matrix. This results in improved molecular entanglement and uniform fiber formation during the electrospinning process, similar to the role played by PVA and chia mucilage<sup>16</sup>.

Nanoemulsions, on the other hand, are colloidal systems consisting of oil, water, and surfactants, with droplet sizes typically ranging between 20 and 200 nm. These systems are highly stable and possess unique physicochemical properties, such as high surface area and low viscosity, making them ideal for encapsulating bioactive compounds<sup>17</sup>. Nanoemulsions enhance the solubility, stability, and bioavailability of encapsulated compounds, offering significant advantages for applications in functional foods, pharmaceuticals, and cosmetics<sup>18</sup>. The small droplet size and uniform distribution of nanoemulsions allow for effective delivery of hydrophobic compounds, such as probiotics and essential oils, across various matrices<sup>19</sup>.

With the increasing interest in functional foods and nutraceuticals, there is a focus on using chia seed-derived hydrocolloids to create novel biomaterials for microencapsulating probiotics. *Bacillus coagulans*, noted for its potential health benefits, including gut microbiome and immune system enhancement, is a key probiotic of interest<sup>20–22</sup>.

This study explores using chia seed hydrocolloids to create nanofiber composites for encapsulating *Bacillus coagulans*. It aims to improve probiotic stability and delivery, with analysis through FTIR and SEM and antioxidant and antimicrobial activity of nanofibers to evaluate their potential in functional foods.

## Experimental Material

Chia seeds (*Salvia hispanica* L.) (Kian Food Company, Tehran, IRAN), Unsaturated sunflower oil rich in vitamin E (Shiraz, Iran), Polyvinyl alcohol (98%), phosphocasein peptide (21%), sodium alginate, resistant corn starch with 99.9% purity, calcium chloride (CaCl<sub>2</sub>), Tween 80 (Merck, Germany), and double-distilled water (DDW) with a purity of 18MΩ cm<sup>−1</sup> from a water purification system (Nanopure Infinity, Barnstead International, Dubuque, IA, USA) were obtained and procured.

### Extraction of Chia seed mucilage

Chia seeds were mixed with NaOH (0.2 M, pH 8) at a 1:20 (w/v) ratio and stirred for 3 h at 1500 rpm using a homogenizer (HD3200, Berlin, Germany) to extract the mucilage. The mixture was then centrifuged (Hettich-320R Universal, Germany) at 4 °C for 20 min to separate swollen seeds and gel. The mucilage was dried at 50 °C for 2 h, ground through a 20 ASTM mesh screen in a mixer (ZONYTEST, Argentina), and stored in polyethylene bags in a cool, dry place<sup>23,24</sup>.

### Antioxidant properties of Chia seed mucilage

The free radical scavenging effect was assessed using the DPPH assay. Four milliliters of extracted chia seed mucilage were added to 100 ml of methanol and incubated at 20 °C for 1 h. Absorbance at 517 nm was measured with a UV-Vis spectrophotometer (Shimadzu UV/Vis-240 IPC, Japan). Antioxidant capacity was calculated using:

$$\text{RSD} = [(A_0 - A)/A_0] \times 100 \quad (1)$$

where %RSD is the free radical scavenging percentage,  $A_0$  is the control absorbance (DPPH solution with DDW), and  $A$  is the sample absorbance (DPPH solution with mucilage)<sup>25</sup>.

### Antimicrobial activity of Chia seed mucilage

The agar diffusion method was used to assess antimicrobial activity. Discs (10 mm diameter) of the samples were prepared and placed on a surface culture inoculated with 100 μL of bacterial suspension containing 10<sup>8</sup> CFU/mL of the tested bacteria, *Staphylococcus aureus* ATCC 25,923 (Gram-positive) and *Escherichia coli* ATCC 25,922 (Gram-negative). The discs were then placed on Muller Hinton agar (Merck, Germany) and incubated at 37 °C for 24 h. Antimicrobial activity was measured by the difference between the disc diameter and the inhibition zone diameter. If no inhibition zone was observed, the antimicrobial activity was recorded as zero<sup>26,27</sup>.

### Electrospinning process

In this experiment, electrospinning was performed on solutions with varying ratios (Table 1) under different conditions: voltages from 12 to 20 kV, feed rates from 0.125 to 0.5 ml/h, and needle-to-collector distances

Sample	Chia Mucilage (%)	Polyvinyl alcohol (%)	Phosphocasein peptide (%)
A	2%	4%	4%
B	3%	4%	4%

**Table 1.** Chia seed mucilage solution samples with different concentrations for electrospinning.

from 9 to 15 cm. For optimization, a constant distance of 9 cm was maintained while varying one parameter at a time and keeping the others constant. This selection was based on initial experiments and previous studies showing that changing the distance had a lesser effect on fiber uniformity than varying voltage and feed rate. The optimization was performed without the use of any specific software, and the results from these experimental conditions were used to determine the best parameters.

After electrospinning, samples were examined using a scanning electron microscope (TESCAN Vega3, Czech Republic) to identify conditions that produced fibers with minimal beads and maximum uniformity. The selected sample was 2% of chia seed mucilage concentration, which was stirred for 15 h at room temperature to form a homogeneous solution and then further homogenized using an ultrasonic titanium probe sonicator (HD3200, Berlin, Germany). The final solution was loaded into a 5-ml syringe and electrospun at 18 kV using an electrospinning device (Full Option Lab 2ESII-II, Iran). The needle-to-collector distance was set to 12 cm, with a collector drum speed of 500 rpm<sup>28</sup>.

**Preparation of *Bacillus coagulans***

Lyophilized *Bacillus coagulans*(ATCC 7050) was obtained from the Scientific and Industrial Research Organization of Iran. It was activated on Nutrient Yeast Extract Salt Medium (NYSM) agar (Merck, Germany) at 37 °C for 24 h. A single colony was then inoculated into NYSM broth and incubated at 37 °C for 48 h with shaking at 250 rpm. The bacterial suspension was centrifuged at 3000×g for 20 min, washed with sterile peptone water, and stored in the refrigerator until use<sup>29</sup>.

**Microencapsulation of *Bacillus coagulans***

The microencapsulation process of *Bacillus coagulans*was carried out by preparing a mixture of sodium alginate (1%) and resistant corn starch (1%) in sterile distilled water. This mixture was stirred with a magnetic stirrer until homogeneous. Ten milliliters of this mixture was added dropwise to 250 mL of sunflower oil containing Tween 80, forming a water-in-oil emulsion. To form microcapsules and break the emulsion, a cold 0.1 M calcium chloride solution was slowly added while stirring for 5 min. The microcapsules were then separated by centrifugation, washed to remove residual oil, and stored in sterile glass containers in a refrigerator for later use<sup>30</sup>.

**Production of nanofibers containing microencapsulated bacteria**

The optimum ratio from the nanofiber preparation stage (Table 1) was used to prepare a solution containing 0.5% encapsulated *Bacillus coagulans*. The bacteria were microencapsulated using a mixture of sodium alginate (1%) and resistant corn starch (1%) as the encapsulating agents. This solution was stirred at 25 °C and then immediately electrospun for 2 h using the electrospinning setup described in Sect. 2.7. The nanofibers were composed of chia seed mucilage, with the encapsulated bacteria included in the final electrospun structure<sup>31</sup>.

**Production of Nanoemulsion containing microencapsulated bacteria**

A 1% solution was prepared from 2% mucilage solution (Table 1), 0.5% of the encapsulated bacteria was added to this solution and stirred at 300 rpm for 10 min, refrigerated for 24 h to fully hydrate, and then mixed with an Ultra-Turrax machine (T18, IKA, Germany) at 10,000 rpm for 1 min<sup>32</sup>.

**Particle size and stability**

The particle size of the samples (nanoemulsion and nanofibers with encapsulated bacteria) was measured using a particle size analyzer (DLS W3325, Microtrac, USA) at 25 °C with Mastersizer 3000 software. Measurements were taken at 2%, 6%, and 10% dilutions to avoid multiple scattering effects<sup>33</sup>. The span was calculated using Eq. 2:

$$\text{Span} = \frac{D(90\%) - D(10\%)}{D(50\%)} \tag{2}$$

where  $D_{90\%}$  is the diameter below which 90% of particles fall,  $D_{50\%}$  is the median diameter,  $D_{10\%}$  is the diameter below which 10% of particles fall.

**Encapsulation efficiency**

One gram of each sample (nanofiber and nanoemulsion with encapsulated bacteria) was suspended in 9 mL of 0.1 M phosphate buffer (pH 7.0) and homogenized with a magnetic stirrer. The viable cell count was determined by serial dilutions plated on MRS agar and incubated at 37 °C for 48 h<sup>34,35</sup>.

$$\text{Encapsulation Efficiency \%} = \frac{\text{amount of encapsulated components (log cfu g}^{-1}\text{)}}{\text{amount of initial components}} \times 100 \tag{3}$$

### Storage Stability of Encapsulated compounds in nanofibers and Nanoemulsion

Storage stability was assessed over 20 days at 7-day intervals (days 0, 7, 14, and 20). For this, 24 mg of nanofibers containing microencapsulated compounds were divided into 12 Eppendorf tubes (2 mg each). The tubes were placed in a desiccator at 33% relative humidity and stored in an oven at 25 °C. On each test day, 2 samples were dissolved in 5% ethanol, filtered using a 0.45 µm needle filter, and their absorbance was measured at 282 nm. A calibration curve was used to determine the concentration of the released compounds from the absorbance readings.

To compare the stability of microencapsulated compounds, 10 µL of the compounds were stored in Eppendorf tubes under the same conditions. At each interval, 2 samples were dissolved in ethanol, and absorbance readings were taken to calculate the release percentage during storage using the release test formula<sup>36,37</sup>.

$$\text{Release \%} = \frac{\text{amount of compound released at time } t}{\text{total amount of encapsulated compound}} \times 100 \quad (4)$$

### Scanning Electron Microscope (SEM)

The surface of nanocomposite samples with varying concentrations of chia seed mucilage was analyzed using a scanning electron microscope (TESCAN vega3, Czech Republic) at 5 kW. Small pieces of the samples were mounted on aluminum holders with silver adhesive and coated with gold for 5 min (DSR1, Nanostructure Coating Co., Iran) in a sputtering device. Imaging was then performed at magnifications up to 20,000x<sup>38</sup>.

### FTIR Spectroscopy

FTIR analysis was conducted using a Spectrum Two FTIR spectrometer (Perkin Elmer, USA). Thin discs of the dried samples (nanofiber and nanoemulsion with encapsulated bacteria), each less than 1 mm thick, were prepared by pressing with potassium bromide in a sample holder. The transmittance spectra were recorded in the wavenumber range of 4000–400 cm<sup>−1</sup> with a resolution of 5 cm<sup>−1</sup><sup>39</sup>.

### Statistical analysis

Measurements were performed in triplicate. Results are reported as mean ± standard deviation (SD). Analysis of variance (ANOVA) was conducted, and significant differences between mean values were assessed using Duncan's multiple range test with a significance level of ( $p < 0.05$ ), analyzed with SAS software (ver. 9.1, SAS Institute Inc., Cary, NC)<sup>40</sup>.

## Results

### Antioxidant activity of Chia seed mucilage

In Fig. 1, the DPPH free radical scavenging ability of chia seed mucilage (*Salvia hispanica* L.) is presented. The results show a concentration-dependent increase in DPPH radical scavenging activity with different concentrations of chia seed mucilage. At the highest concentration tested (350 µg/mL), the chia seed mucilage exhibited a significant DPPH radical scavenging activity of 67.88%. The increasing IC<sub>50</sub> values with higher concentrations reflect the cumulative effect of the mucilage in neutralizing DPPH radicals, indicating that higher concentrations are necessary to achieve the same level of radical inhibition as the mucilage concentration increases.

### Antimicrobial activity of Chia seed mucilage

The inhibition zone (ZOI) diameters obtained by the disc diffusion method for the Gram-positive (*Staphylococcus aureus*) and Gram-negative (*Escherichia coli*) bacteria are presented in Fig. 2. The data indicate that chia seed mucilage exhibits moderate antimicrobial activity against both *Staphylococcus aureus* and *Escherichia coli*, with inhibition zones of 9 mm and 6 mm, respectively. However, the antimicrobial efficacy of the mucilage is significantly lower than that of the antibiotics tested. The findings of this investigation showed the higher sensitivity of gram-positive bacteria compared to gram-negative bacteria that can be attributed to the absence of a lipopolysaccharide cell wall in gram-positive bacteria. This structural difference in the cell wall composition is likely a contributing factor to the enhanced susceptibility of gram-positive bacteria to the antimicrobial properties of the chia seed mucilage<sup>41,42</sup>.

### Morphology of Mucilage Fiber

Nanofibers of mucilage were examined using scanning electron microscopy at different concentrations. The nanofibers produced at concentrations of 2% and 3% exhibited distinct morphologies, as observed in the SEM images (Fig. 3a and b). The average diameter of the nanofibers at 3% mucilage concentration (Fig. 3a) was approximately 26.24 µm, showing a flat and uniform structure. Conversely, the nanofibers at 2% mucilage concentration (Fig. 3b) had a significantly thinner diameter of approximately 12.36 µm. These thinner fibers are attributed to the lack of solvent evaporation between the nozzle tip and the collector, owing to the high fluid jet diameter<sup>43</sup>. As shown in Fig. 3a and b, the variation in fiber diameters suggests successful formation of hybrid membranes with interwoven structures, when fibers of different diameters overlap<sup>44–46</sup>. These findings demonstrate adequate molecular entanglement for producing defect-free fibers in electrospinning solutions.

### Microencapsulation efficiency of Bacteria

The encapsulation efficiency of the nanocomposite containing encapsulated *Bacillus coagulans* was significantly higher than that of the nanoemulsion containing encapsulated *Bacillus coagulans* ( $p < 0.05$ ), as shown in Table 2. Several factors, such as the type of nanocomposite, the solution composition, the encapsulation process, and

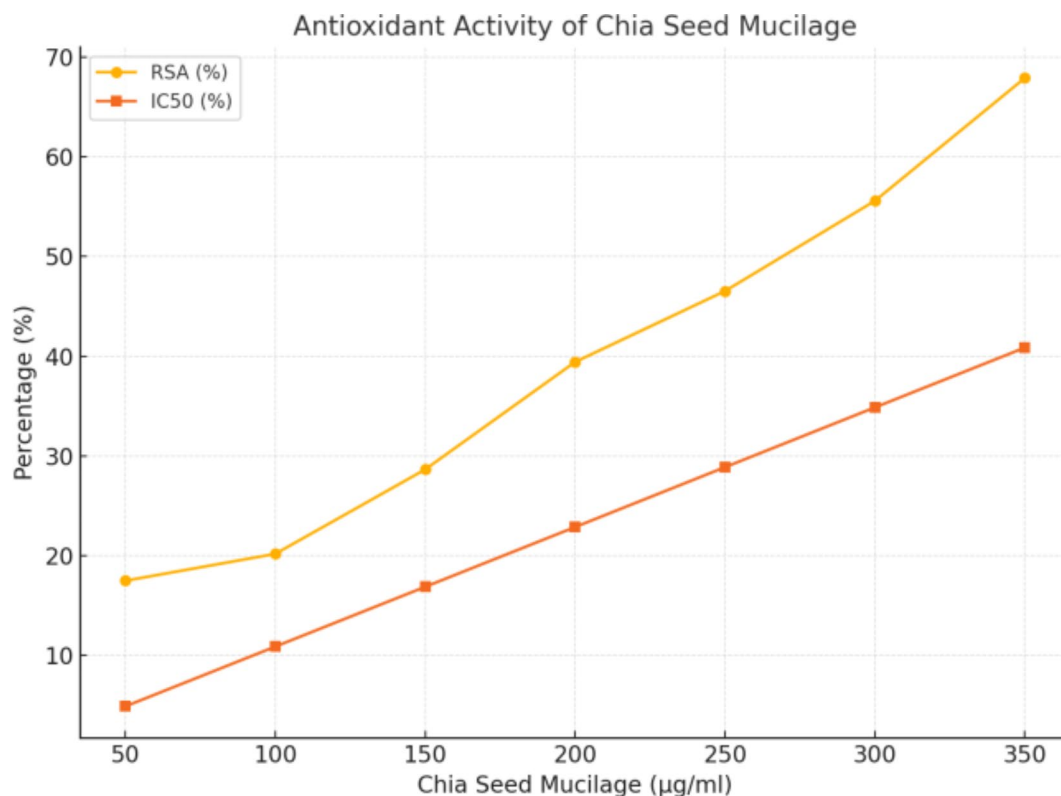


**Fig. 1.** DPPH radical inhibition evaluation of chia seed mucilage.

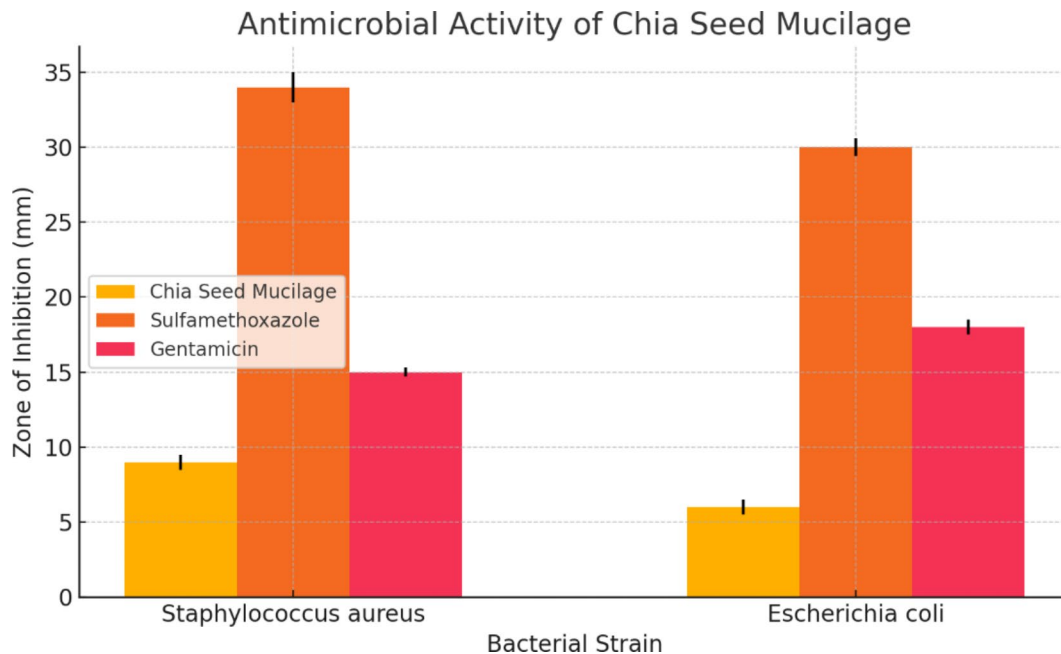


**Fig. 2.** DPPH radical inhibition evaluation of chia seed mucilage.

the test conditions, influence the encapsulation efficiency of the nanocomposite solution. The encapsulation efficiency of *Bacillus coagulans* influenced by several factors. The type of nanocomposite plays a critical role by providing enhanced mechanical stability and stronger interactions between the microcapsules and the fibrous matrix, reducing leakage. The solution composition, including chia seed mucilage, sodium alginate, and resistant corn starch, forms a stable network that creates a protective environment for the bacteria. The



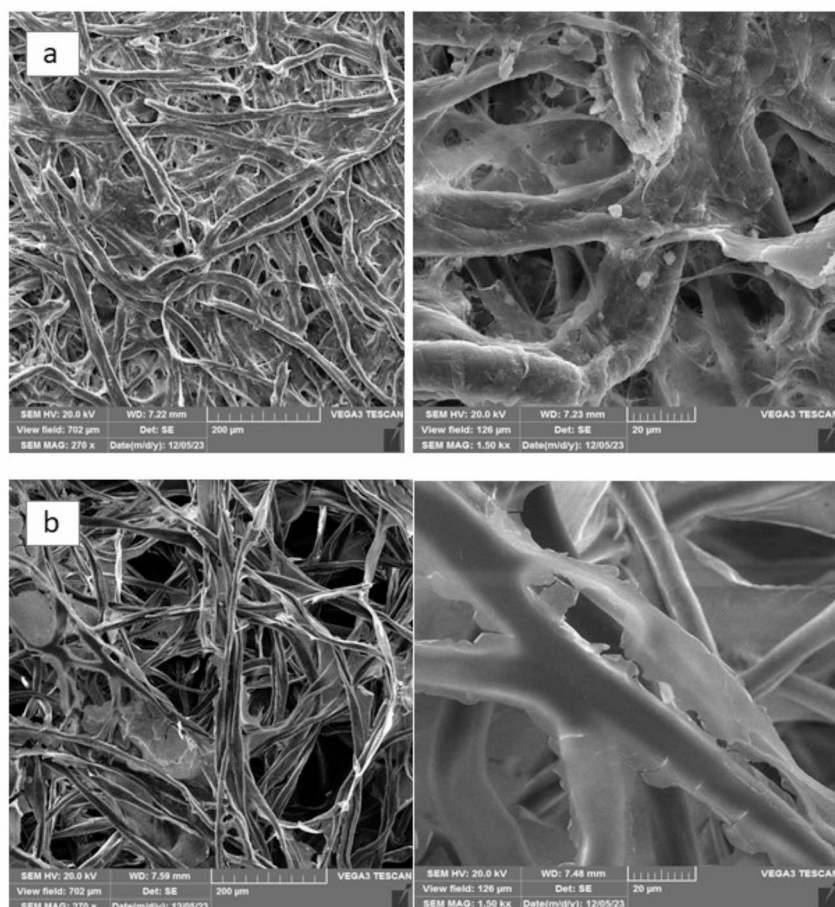


**Fig. 3.** Morphology of fiber with (a) 3% chia seed mucilage (b) 2% chia seed mucilage.

Sample	Efficiency (%)
Nanoemulsion containing encapsulated <i>Bacillus coagulans</i>	88.33 ± 2.00 <sup>b</sup>
Electrospun nanocomposite containing encapsulated <i>Bacillus coagulans</i>	93.90 ± 2.10 <sup>a</sup>

**Table 2.** Microencapsulation efficiency of *Bacillus coagulans* in Nanofiber and Nanoemulsion. The results are presented in the form of mean ± standard deviation for each of the treatments, and all experiments were performed in three repetitions. Values with different letters are significantly different from each other at the 5% level.

encapsulation process, particularly electrospinning, ensures uniform distribution of microcapsules within the nanofiber matrix, leading to improved efficiency compared to emulsification methods. Additionally, controlled test conditions, such as humidity and temperature, help maintain the integrity of the microcapsules, further enhancing encapsulation efficiency<sup>47</sup>.

### Particle size

In Table 3, the average particle size and particle dispersion index of the encapsulated nanoemulsion and nanofiber were exhibited. No significant difference was observed in the average particle size between the treatments ( $p > 0.05$ ). However, the average particle size in the nanoemulsion containing encapsulated bacteria was larger than that in the electrospun nanocomposite containing encapsulated bacteria. In contrast, the analysis of the particle dispersion index revealed a significant difference between the treatments ( $p < 0.05$ ). The particle dispersion index was significantly higher in the electrospun nanocomposite containing encapsulated bacteria compared to the nanoemulsion treatment ( $p < 0.05$ ). Increasing in concentration (3%) of the mucilage solution and the constant percentage of polyvinyl alcohol (4%) and phosphocasein (4%) significantly increases

Sample	Average particle size (nm)	Particle dispersion index(nm)
Nanoemulsion containing encapsulated <i>Bacillus coagulans</i>	705.2 ± 70.00 <sup>a</sup>	1.1 ± 0.05 <sup>b</sup>
Electrospun nanocomposite containing encapsulated <i>Bacillus coagulans</i>	676 ± 60.00 <sup>a</sup>	1.41 ± 0.1 <sup>a</sup>

**Table 3.** Particle size and particle dispersion index of Nanofiber and Nanoemulsion containing encapsulated *Bacillus coagulans*. The results are presented in the form of mean ± standard deviation for each of the treatments, and all experiments were performed in three repetitions. Values in each column with different letters are significantly different from each other at the 5% level.

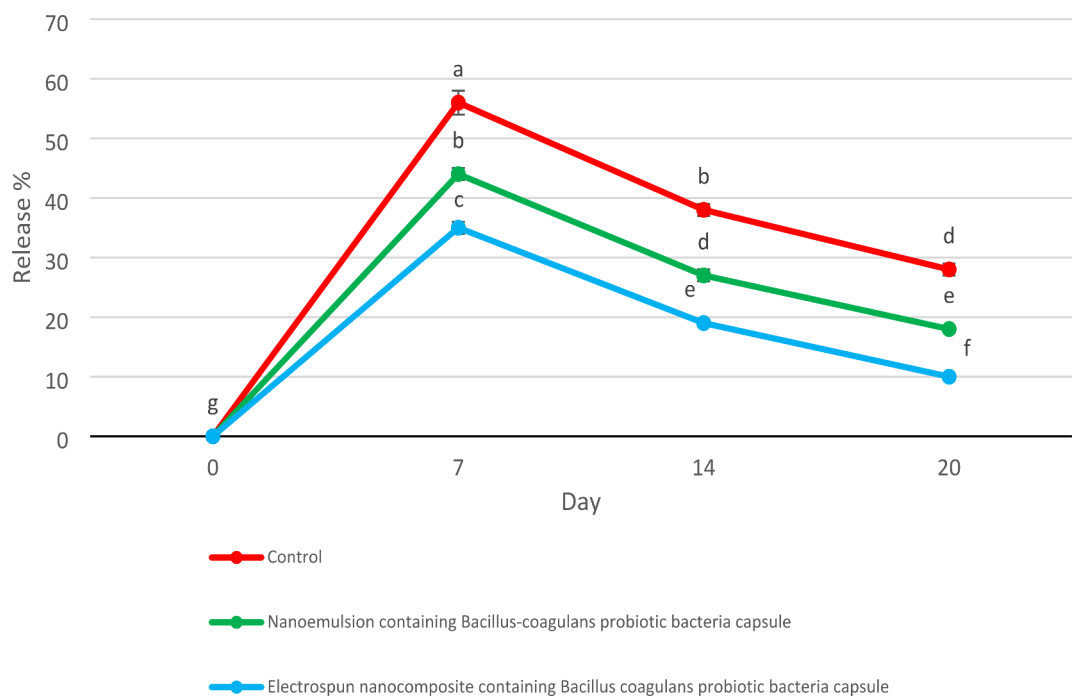


**Fig. 4.** Storage stability of microencapsulated compound in nanofiber and nanoemulsion. Control is encapsulated bacteria before embedding in Nanoemulsion or Nanofiber.

the diameter of the nanofibers. The sample containing chia seed mucilage, peptide-protein phosphocasein, and polyvinyl alcohol showed this increase in nanofiber diameter due to the increase in the viscosity of the polymer solution<sup>48,49</sup>.

### Storage Stability

Figure 4 presents the storage stability results of encapsulated bacteria based on the release percentage in nanofibers and nanoemulsions. A significant difference was observed between the treatments ( $p < 0.05$ ). On the day of production, the release levels were similar across all treatments. However, on subsequent days, the highest release rates were observed in the control group (encapsulated bacteria before embedding in nanoemulsion or nanofiber), followed by the nanoemulsion, and finally, the electrospun nanocomposite. The release rate increased for all treatments by the 7th day, after which it gradually decreased until the end of the study period. The control group exhibited the highest release rate ( $56.00 \pm 2.00$ ) on the 7th day, with a notably rapid release occurring in the first seven days. The high release rates of encapsulated compounds may be attributed to the hydrocolloid matrix and surface interaction with phosphocasein proteins<sup>50,51</sup>. Our findings demonstrated that the encapsulation efficiency and storage stability of *Bacillus coagulans* was significantly higher in nanofibers compared to nanoemulsions, attributed to the structural advantages and protective environment provided by the nanofiber matrix.

### Morphology of Encapsulated Nanofiber and Nanoemulsion

Scanning Electron Microscopy (SEM) was employed to examine several properties of the nanoparticles and encapsulated bacteria, including surface morphology, structural integrity, and the internal cross-sectional view of the bacterial microcapsules. In Fig. 5a, the surface morphology of the encapsulated *Bacillus coagulans* shows uniformity and structural integrity in the microcapsules. Figure 5b highlights the encapsulation of bacteria within the nanoemulsion matrix, where the smooth and homogeneous texture suggests effective encapsulation and stability in the emulsion environment. Figure 5c demonstrates the incorporation of encapsulated bacteria

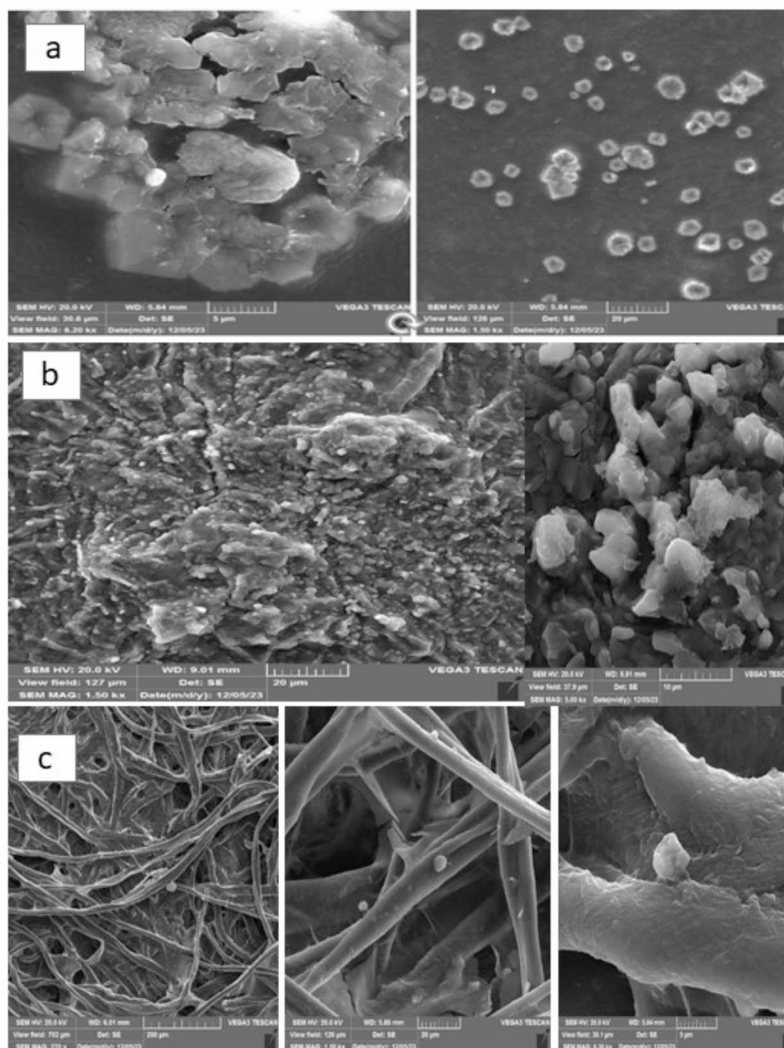


**Fig. 5.** Morphology of (a) Encapsulated *Bacillus coagulans* (b) Encapsulated *Bacillus coagulans* embedded in nanoemulsion and (c) Encapsulated *Bacillus coagulans* embedded in nanofiber.

into electrospun nanofibers, revealing a fibrous and porous structure that provides a protective environment, enhances stability, and supports controlled release. These observations confirm the successful integration of *Bacillus coagulans* into the designed delivery systems, highlighting their potential for improved stability and bioactivity.

### FTIR

Considering that the electrospun product contains encapsulated components from *Bacillus coagulans* bacteria, chia mucilage, polyvinyl alcohol, and phosphocasein peptides, the peaks observed in Fig. 6 in the range of 1500 to 2000  $\text{cm}^{-1}$  correspond to the stretching vibrations of C=O (1650–1750  $\text{cm}^{-1}$ ), which arise from the presence of carbonyl groups in the structures of compounds such as peptides (proteins) and lipids. The peaks related to the stretching vibrations of C=C (1500–1600  $\text{cm}^{-1}$ ) are due to the presence of double bonds in aromatic rings found in some compounds. In the range of 3000 to 3500  $\text{cm}^{-1}$ , the peaks associated with the stretching vibrations of O-H (3200–3500  $\text{cm}^{-1}$ ) indicate the presence of hydroxyl groups in the structures of compounds like polyvinyl alcohol, chia mucilage, and phosphocasein peptides. Additionally, the peaks related to the stretching vibrations of N-H (3300–3500  $\text{cm}^{-1}$ ) indicate the presence of amine groups in the structure of peptides and proteins. In the range of 500 to 1000  $\text{cm}^{-1}$ , the peaks corresponding to the stretching vibrations of C-O (1000–1200  $\text{cm}^{-1}$ ) are attributed to the presence of ether and ester groups in the structures of compounds such as polyvinyl alcohol and phosphopeptides. The peaks associated with the C-C vibrations (500–800  $\text{cm}^{-1}$ ) result from the presence of carbon-carbon bonds in the structure of organic compounds. In the range of 2000 to 2500  $\text{cm}^{-1}$ , the peaks related to the vibrations of C≡N (2200–2300  $\text{cm}^{-1}$ ) suggest the presence of nitrile groups in the structure of certain compounds, while the peaks corresponding to C≡C vibrations (2100–2250  $\text{cm}^{-1}$ ) indicate the presence of triple carbon-carbon bonds in the structure of some compounds<sup>14,22</sup>. Given that the electrospun product



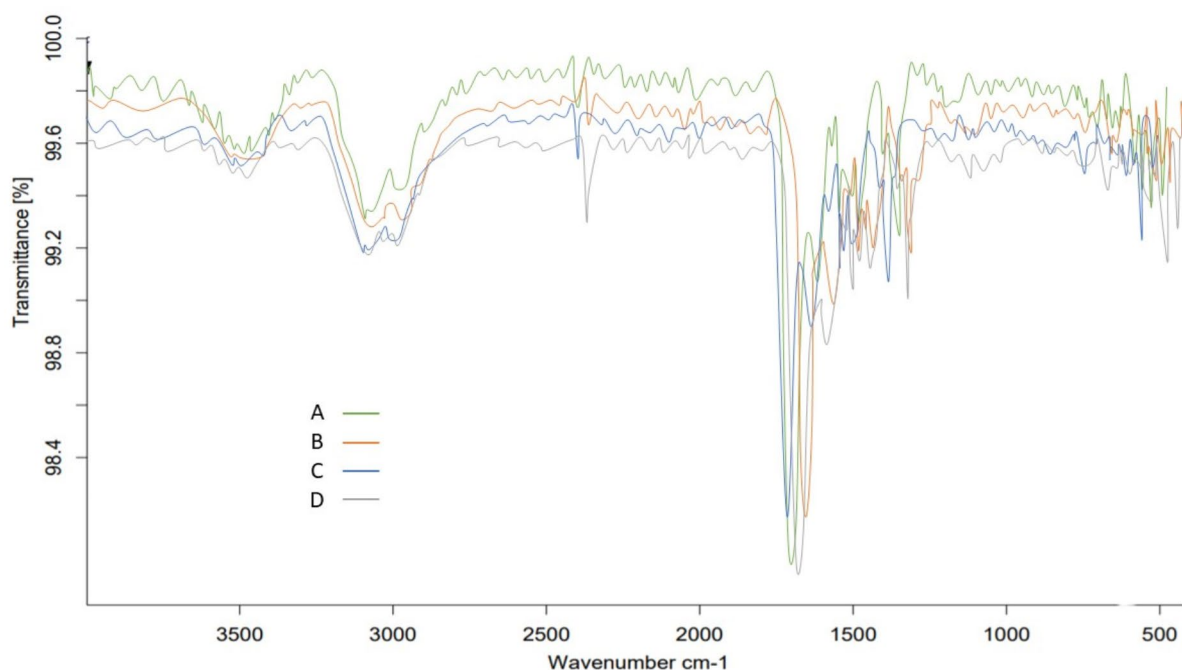


**Fig. 6.** FTIR analysis of (A) Encapsulated *Bacillus coagulans* embedded in nanoemulsion (B) Encapsulated *Bacillus coagulans* embedded in Nanofiber (C) Nanoemulsion (D) Non-capsulated *Bacillus coagulans* embedded in nanoemulsion.

utilizes *Bacillus coagulans* bacteria, it is expected that the FT-IR spectrum of this product will show some peaks corresponding to the chemical structure of this bacterium. The peaks in the range of  $1500\text{--}1600\text{ cm}^{-1}$  correspond to the stretching vibrations of C=C bonds in the aromatic rings present in the structure of *Bacillus coagulans*. The range of  $2800\text{--}3000\text{ cm}^{-1}$  is associated with the stretching vibrations of C-H in the methyl and methylene groups found in the fatty acids and proteins of the bacterium. The  $1650\text{--}1750\text{ cm}^{-1}$  range corresponds to the stretching vibrations of C=O in the carbonyl groups within the bacterial proteins. The peaks in the range of  $1540\text{--}1560\text{ cm}^{-1}$  are related to the N-H bending vibrations in the amide (peptide) groups present in the bacterial proteins, while the  $1200\text{--}1400\text{ cm}^{-1}$  range corresponds to the stretching vibrations of C-N in the amine groups found in the amino acids that make up the bacterial proteins. Additionally, peaks in the  $3200\text{--}3500\text{ cm}^{-1}$  range, associated with the stretching vibrations of O-H, indicate the presence of hydroxyl groups in the extracellular polysaccharides produced by *Bacillus coagulans*<sup>52–54</sup>. FTIR analysis further confirmed the successful encapsulation of *Bacillus coagulans* within the nanofiber matrix, with characteristic peaks corresponding to both the bacterial and chia seed mucilage components. These findings suggest that electrospun nanofibers, integrating chia seed mucilage and *Bacillus coagulans*, offer a viable method for creating stable, bioactive, and functional encapsulation systems, with potential applications in various industries, including food, pharmaceuticals, and cosmetics.

## Discussion

The DPPH free radical scavenging effects of hydrocolloids have been extensively studied, highlighting their bioactive and antioxidant properties. Hydrocolloids, which include both polysaccharides and proteins, demonstrate significant antioxidant activities<sup>55,56</sup>. Polysaccharide-based hydrocolloids, in particular, have been shown to effectively scavenge and neutralize free radicals, such as the DPPH radical, through various mechanisms. One key mechanism involves enhancing the superoxide dismutase (SOD) content, thereby supporting the overall antioxidant defense system<sup>57</sup>. The findings from this study indicate that chia seed mucilage is a rich source of natural antioxidants, capable of efficiently scavenging and neutralizing harmful free radicals. The high antioxidant activity observed in chia seed mucilage is likely due to the presence of polyphenolic compounds, vitamins, and other bioactive constituents within the mucilage matrix<sup>58</sup>. Caffeic and chlorogenic acids are the primary phenolic compounds found in chia seeds. These compounds play a crucial role in defending against free radicals and inhibiting the peroxidation of fats, proteins, and DNA<sup>25</sup>. These results suggest the potential of chia seed mucilage as a valuable functional ingredient in the development of antioxidant-rich food, pharmaceutical, and cosmetic products<sup>58–61</sup>. The antioxidant activity of chia seed mucilage, with its high DPPH radical scavenging capacity, underscores its role as a natural antioxidant source. The moderate antibacterial activity observed for chia seed mucilage suggests that it may contain bioactive compounds capable of inhibiting bacterial growth, though not as effectively as gentamicin or sulfamethoxazole. The smaller inhibition zones, particularly against *E. coli*, may reflect the mucilage's lower potency or a different mechanism of action compared to these antibiotics. The results indicate the potential for chia seed mucilage as a supplementary antimicrobial agent, possibly in

combination with other treatments. However, its relatively low efficacy compared to standard antibiotics suggests that it may be more appropriate for applications where mild antimicrobial activity is sufficient, or where natural or plant-based antimicrobials are preferred<sup>62,63</sup>. The antimicrobial analysis revealed moderate efficacy, particularly against Gram-positive bacteria, suggesting that chia seed mucilage could be utilized as a supplementary antimicrobial agent. Previous studies have shown that when the viscosity of the electrospinning solution decreases from 0.453 to 0.118 Pa.s, sufficient intermolecular entanglement occurs, preventing the fiber jet from breaking into droplets and resulting in higher-quality fibers. Our results align with these findings, as reducing the mucilage concentration—and consequently the viscosity—enhanced molecular entanglement in the 2% electrospinning solution, thereby improving the spinning properties of the fibers. Moreover, the extremely thin fiber diameter was influenced by the combined effects of solution viscosity and electrical conductivity<sup>64</sup>. Encapsulation efficiency refers to the amount and quality of the encapsulated material within the nanocomposite. Parameters such as the percentage of encapsulation and particle size distribution are commonly used to assess this efficiency<sup>30,65</sup>. Alginate and corn starch were selected as encapsulating materials due to their unique physicochemical properties and their proven effectiveness in probiotic encapsulation systems. Alginate is widely recognized for its excellent gel-forming ability, biocompatibility, and protective properties, which help to shield probiotics from environmental stresses such as pH variations and high temperatures. Its ability to form a stable gel matrix ensures uniform distribution of probiotics and enhances encapsulation efficiency, as supported by previous studies<sup>66</sup>. Corn starch, on the other hand, acts as a filler and structural support, improving the mechanical stability of the encapsulation matrix. It also contributes to controlled release properties by slowing down the diffusion of probiotics, thus enhancing their stability during storage. Moreover, the polysaccharide structure of corn starch can create a prebiotic effect, indirectly promoting probiotic growth and activity during gastrointestinal transit<sup>49,67</sup>. The combination of alginate and corn starch in this study was aimed at leveraging their complementary properties. The higher encapsulation efficiency of microencapsulated *Bacillus coagulans* fibers, compared to nanoemulsions, is likely due to the enhanced mechanical stability, stronger interaction between the microcapsules and the fibrous matrix, better environmental protection, and more controlled release properties offered by the fibrous structure. These factors collectively contribute to the superior performance of fibers as carriers for microencapsulated bacteria<sup>68,69</sup>. Similar findings were reported by Nawaz et al. (2023), who demonstrated an encapsulation efficiency of 82.90% for *Lactobacillus acidophilus* encapsulated in apple pectin/PVA nanofibers. They attributed the high EE% to the uniform distribution of probiotics within the nanofiber structure, facilitated by the solubility and mechanical properties of the biopolymer matrix. The strong and flexible biopolymer matrix in nanofibers, as discussed by Nawaz et al. (2023), ensures enhanced structural integrity and protection of probiotics from external stresses, such as shear forces. This aligns with our findings, as the nanofiber matrix in our study not only provided better encapsulation efficiency but also maintained the stability and controlled release of *Bacillus coagulans* over the storage period<sup>70</sup>. These results further highlight the advantages of nanofiber-based encapsulation systems compared to other delivery systems, such as nanoemulsions. Moreover, Nawaz et al. (2023) and other studies, such as those by Ma et al. and Simonič et al., have also reported that biopolymers like gum Arabic, sodium alginate, and polyethylene oxide contribute to the successful encapsulation of probiotics, primarily due to their compact structure and biocompatibility<sup>71,72</sup>. The results of our study are consistent with these findings, indicating that the choice of biopolymer and encapsulation method plays a critical role in improving encapsulation efficiency and maintaining probiotic viability. The nanoemulsion system in our study demonstrated moderate encapsulation efficiency and probiotic viability for *Bacillus coagulans* during storage, which aligns with findings from previous studies. For example, Vaishnavi et al. (2020) reported that nanoemulsions prepared using soy protein and gum Arabic effectively enhanced the stability and survivability of *Lactobacillus delbrueckii* subsp. *bulgaricus* during 40 days of storage. They observed a consistent viable count for the first 15 days, followed by an increase in viability, attributed to the prebiotic properties of gum Arabic and the growth-promoting effects of soy protein. The stability and viability of probiotics in nanoemulsions are highly dependent on the matrix components and their ability to protect probiotics against external stresses<sup>73</sup>. Similar to Vaishnavi et al. (2020), our findings suggest that nanoemulsions can act as a suitable delivery system for probiotics, although their long-term stability and encapsulation efficiency remain lower compared to nanofibers. This is likely due to the structural differences between the two systems, as nanofibers offer a more compact and protective matrix. The differences in particle size and dispersion index between the nanoemulsion and electrospun nanocomposite are likely due to the inherent differences in the encapsulation environments and stabilization mechanisms provided by these two systems. The electrospun nanocomposite, with its solid and stable matrix, offers superior control over particle size and distribution, leading to a more uniform dispersion of encapsulated bacteria. This contrasts with the nanoemulsion, where the liquid medium and potential for instability can result in less consistent particle sizes and distribution. These findings suggest that electrospinning is a more effective technique for achieving stable and uniform encapsulation of bacterial particles compared to nanoemulsion methods<sup>74,75</sup>. The high release rates of encapsulated compounds may be attributed to the hydrocolloid matrix and surface interaction with phosphocasein proteins<sup>50,51</sup>. Our findings demonstrated that the encapsulation efficiency and storage stability of *Bacillus coagulans* were significantly higher in nanofibers compared to nanoemulsions, attributed to the structural advantages and protective environment provided by the nanofiber matrix. The presence of wrinkles and cracks is likely due to the drying process employed during the preparation of the microcapsule powder. Additionally, crystalline, grain-like structures were commonly observed in figures. These crystal-like formations are a result of the capsule preparation process, specifically due to the drying method used<sup>76–78</sup>. The morphological characteristics of the nanofibers produced, especially at lower concentrations, demonstrated adequate molecular entanglement, contributing to defect-free fiber production. The study by Madybekova et al. (2024) investigated the development of probiotic delivery systems co-encapsulated with plant extracts, aimed at enhancing survivability, prolonging nutritional benefits, and enriching fermented beverages based on acid whey. They utilized FTIR analysis to identify functional groups in

microcapsules containing *Bifidobacterium bifidum* and stevia extract. Their findings revealed shifts in key peaks, such as  $3413.9\text{ cm}^{-1}$  (NH stretching),  $1650\text{ cm}^{-1}$  (CO stretching), and  $2127\text{ cm}^{-1}$  (nitrile groups), indicating significant interactions between the encapsulated agents and wall materials like alginate and chitosan. Similarly, in the present study, FTIR spectra confirmed the presence of characteristic functional groups, such as C=O, C=C, and O-H stretching vibrations, in nanoemulsion-based edible films encapsulating *Bacillus coagulans* and chia seed mucilage. These results suggest the successful formation of stable bonds within the matrix, aligning with the findings of Madybekova et al., and further validating the effectiveness of the encapsulation system<sup>79</sup>. The study by Krithika and Preetha (2019) investigated the physicochemical properties and stability of synbiotic nanoemulsions, utilizing FTIR spectroscopy to monitor structural changes in the emulsion system. Similar results were observed in our study, particularly in the bands associated with C=O stretching vibrations, which indicate changes in the protein structure and other components in the emulsion system. These findings highlight that FTIR is an effective tool for evaluating the stability and molecular changes in nanoemulsion systems<sup>80</sup>. The results of this study demonstrated the successful encapsulation of *Bacillus coagulans* within an electrospun nanofiber matrix and provided detailed insights into the chemical interactions of the encapsulated components. In comparison, the study by Alizadeh et al. also identified key functional groups such as carbonyl (C=O) and hydroxyl (O-H) groups, confirming the structural contributions of proteins, polysaccharides, and other bioactive compounds. However, this study offers additional observations, including the presence of nitrile groups (C≡N) within the nanofiber matrix, which were not reported by Alizadeh et al. This difference could be attributed to variations in the composition of the encapsulated materials or the specific methodologies employed. Furthermore, the identification of C-H stretching vibrations in fatty acids and proteins, as well as amide and amine groups from bacterial proteins, highlights the unique contributions of *Bacillus coagulans* and its extracellular components in this system. The comparison underscores the enhanced analytical approach in this study, which not only validates the findings of Alizadeh et al. but also expands on them by identifying additional functional groups and molecular interactions. These differences reflect the broader applicability and versatility of the encapsulation system developed in this research for delivering bioactive compounds in various industries<sup>81</sup>. These findings suggest that electrospun nanofibers, integrating chia seed mucilage and *Bacillus coagulans*, offer a viable method for creating stable, bioactive, and functional encapsulation systems, with potential applications in various industries, including food, pharmaceuticals, and cosmetics.

## Conclusion

This study highlights the potential of chia seed mucilage and *Bacillus coagulans* in the development of functional food and pharmaceutical products, emphasizing the effectiveness of composite nanofibers for encapsulating probiotics. The antioxidant and antimicrobial properties of chia seed mucilage, as well as its ability to form stable nanofibers, make it a promising candidate for encapsulation purposes. Our findings demonstrated that the encapsulation efficiency and storage stability of *Bacillus coagulans* were significantly higher in nanofibers compared to nanoemulsions, attributed to the structural advantages and protective environment provided by the nanofiber matrix. Moreover, the morphological analysis confirmed that nanofibers offer better control over the encapsulated bacteria's morphology, ensuring improved encapsulation efficiency and stability. The antioxidant activity of chia seed mucilage, with its high DPPH radical scavenging capacity, underscores its role as a natural antioxidant source. Although the antimicrobial activity of chia seed mucilage was moderate, its efficacy against Gram-positive bacteria suggests potential as a supplementary antimicrobial agent. This moderate activity, when combined with other antimicrobial agents, could enhance overall product protection. Furthermore, it may be suitable for use in formulations where mild antimicrobial action is sufficient, such as in low-risk food products or as part of a multi-barrier preservation strategy. The morphological characteristics of the nanofibers produced, especially at lower concentrations, demonstrated adequate molecular entanglement, contributing to defect-free fiber production. FTIR analysis further confirmed the successful encapsulation of *Bacillus coagulans* within the nanofiber matrix, with characteristic peaks corresponding to both the bacterial and chia seed mucilage components. These findings suggest that electrospun nanofibers, integrating chia seed mucilage and *Bacillus coagulans*, offer a viable method for creating stable, bioactive, and functional encapsulation systems, with potential applications in various industries, including food, pharmaceuticals, and cosmetics. Additional studies are being conducted to evaluate the application of encapsulated *Bacillus coagulans* in food products, focusing on its functional and sensory properties. These investigations aim to further explore the potential of this encapsulation system in enhancing product quality and consumer acceptance.

## Data availability

The data that supports the findings of this study is available from the corresponding author upon reasonable request.

Received: 9 October 2024; Accepted: 21 January 2025

Published online: 01 April 2025

## References

1. Singh, T. et al. Application of nanotechnology in food science: perception and overview. *Front. Microbiol.* **8**, 1501 (2017).
2. Jagtiani, E. Advancements in nanotechnology for food science and industry. *Food Front.* **3** (1), 56–82 (2022).
3. Kiss, É. Nanotechnology in food systems: a review. *Acta Aliment.* **49** (4), 460–474 (2020).
4. Thiruvengadam, M., Rajakumar, G. & Chung, I. M. *Nanotechnology: Curr. uses Future Appl. food Ind. 3 Biotech.*, **8**: 1–13. (2018).
5. Berekaa, M. M. Nanotechnology in food industry; advances in food processing, packaging and food safety. *Int. J. Curr. Microbiol. Appl. Sci.* **4** (5), 345–357 (2015).

6. Patel, A. et al. *Application of nanotechnology in the food industry: present status and future prospects*. Impact of nanoscience in the food industry, : pp. 1–27. (2018).
7. Zhu, W. et al. Improving the hydrophobicity and mechanical properties of starch nanofibrous films by electrospinning and cross-linking for food packaging applications. *Lwt* **169**, 114005 (2022).
8. Jankowska, K. et al. *The Impact of Electrospinning Conditions on the Properties of Enzymes Immobilized on Electrospun Materials: Exploring Applications and Future Perspectives*. 103408 (Environmental Technology & Innovation, 2023).
9. Afshari, E. et al. Surface modification of polyvinyl alcohol/malonic acid nanofibers by gaseous dielectric barrier discharge plasma for glucose oxidase immobilization. *Appl. Surf. Sci.* **385**, 349–355 (2016).
10. Ziyadi, H. et al. An investigation of factors affecting the electrospinning of poly (vinyl alcohol)/kefir composite nanofibers. *Adv. Compos. Hybrid. Mater.* **4**, 768–779 (2021).
11. Hoseyni, S. Z. et al. Production and characterization of catechin-loaded electrospun nanofibers from Azivash gum-polyvinyl alcohol. *Carbohydr. Polym.* **235**, 115979 (2020).
12. Alonso-González, M. et al. Developing active poly (vinyl alcohol)-based membranes with encapsulated antimicrobial enzymes via electrospinning for food packaging. *Int. J. Biol. Macromol.* **162**, 913–921 (2020).
13. Dehghani, S. et al. Fabrication and physicochemical characterization of electrospun nanofibers using Chia seed mucilage. *J. Food Bioprocess. Eng.* **6** (1), 1–7 (2023).
14. Dehghani, S. et al. Electrospun Chia seed mucilage/PVA encapsulated with green cardamom essential oils: antioxidant and antibacterial property. *Int. J. Biol. Macromol.* **161**, 1–9 (2020).
15. Coban, O. E. & Jamshidi, A. Development of bionanocomposite film based on Chia seed mucilage incorporated with ZnO nanoparticles and their application for preserving fresh rainbow trout (*Oncorhynchus mykiss*) fillets. *J. Food Meas. Charact.* **18** (2), 1000–1011 (2024).
16. Tenenbaum, M. et al. Identification, production and bioactivity of casein phosphopeptides—A review. *Food Res. Int.* **157**, 111360 (2022).
17. Preeti et al. Nanoemulsion: an emerging novel technology for improving the bioavailability of drugs. *Scientifica* **2023** (1), 6640103 (2023).
18. Kapoor, D. U. et al. The potential of Quality Target Product Profile in the optimization of Nanoemulsions. *Curr. Nanomed.* **15** (1), 4–17 (2025).
19. Mushtaq, A. et al. *Recent Insights into Nanoemulsions: Their Preparation, Properties and Applications* 18p. 100684 (X, 2023).
20. Tekin, M. D., Celikozlu, S. & Aydin, H. Electrospun rocket seed (*Eruca sativa* Mill) mucilage/polyvinyl alcohol nanofibers: fabrication and characterization. *Iran. Polym. J.* **32** (2), 203–211 (2023).
21. Golkar, P. et al. Fabrication and characterization of electrospun Plantago major seed mucilage/PVA nanofibers. *J. Appl. Polym. Sci.* **136** (32), 47852 (2019).
22. de Paiva, P. H. E. N. et al. Film production with flaxseed mucilage and polyvinyl alcohol mixtures and evaluation of their properties. *J. Food Sci. Technol.* **58**, 3030–3038 (2021).
23. Tavares, L. S. et al. Cold extraction method of Chia seed mucilage (*Salvia hispanica* L.): effect on yield and rheological behavior. *J. Food Sci. Technol.* **55**, 457–466 (2018).
24. Silva, L. et al. Extraction of Chia seed mucilage: effect of ultrasound application. *Food Chem. Adv.* **1**, 100024 (2022).
25. Atik, D. S. et al. Chia seed mucilage versus guar gum: effects on microstructural, textural, and antioxidative properties of set-type yoghurts. *Brazilian Archives Biology Technol.* **63**, e20190702 (2020).
26. Khodaman, E. et al. Production and evaluation of physicochemical, mechanical and antimicrobial properties of Chia (*Salvia hispanica* L.) mucilage-gelatin based edible films incorporated with chitosan nanoparticles. *J. Food Meas. Charact.* **16** (5), 3547–3556 (2022).
27. Mahajan, P. et al. Chia (*Salvia hispanica* L.) seed mucilage (a heteropolysaccharide) based antimicrobial hydrogel scaffold for wound healing: in vitro-in-vivo characterization. *Carbohydr. Polym. Technol. Appl.* **7**, 100432 (2024).
28. Bavatharani, C. et al. Electrospinning technique for production of polyaniline nanocomposites/nanofibres for multi-functional applications: a review. *Synth. Met.* **271**, 116609 (2021).
29. Fayed, R., Elnemr, A. M. & El-Zahed, M. M. Synthesis, characterization, antimicrobial and electrochemical studies of biosynthesized zinc oxide nanoparticles using the probiotic *Bacillus coagulans* (ATCC 7050). *J. Microbiol. Biotechnol. food Sci.* **13** (3), e9962–e9962 (2023).
30. Pandey, K. R. & Vakil, B. V. Encapsulation of probiotic bacillus coagulans for enhanced shelf life. *J. Appl. Biol. Biotechnol.* **5**, 57–65 (2017).
31. Panahi, Z., Mohsenzadeh, M. & Hashemi, M. Fabrication and characterization of PVA/WPI nanofibers containing probiotics using electrospinning technique. *Nanomed. J.*, **10**(3), 216–226 (2023).
32. Rao, J. & McClements, D. J. Formation of flavor oil microemulsions, nanoemulsions and emulsions: influence of composition and preparation method. *J. Agric. Food Chem.* **59** (9), 5026–5035 (2011).
33. García-Moreno, P. J. et al. Encapsulation of fish oil in nanofibers by emulsion electrospinning: physical characterization and oxidative stability. *J. Food Eng.* **183**, 39–49 (2016).
34. Rama, G. R. et al. Ricotta whey supplemented with gelatin and collagen for the encapsulation of probiotic lactic acid bacteria. *Food Sci. Technol.* **41**, 576–586 (2020).
35. de Andrade, D. P. et al. Stability of microencapsulated lactic acid bacteria under acidic and bile juice conditions. *Int. J. Food Sci. Technol.* **54** (7), 2355–2362 (2019).
36. Postružnik, V. et al. Impact of Storage conditions on Stability of Bioactive compounds and Bioactivity of Beetroot Extract and Encapsulates. *Processes* **12** (7), 1345 (2024).
37. Jia, C. et al. Storage stability and in-vitro release behavior of microcapsules incorporating fish oil by spray drying. *Colloids Surf., a.* **628**, 127234 (2021).
38. Campano, C. et al. A reproducible method to characterize the bulk morphology of cellulose nanocrystals and nanofibers by transmission electron microscopy. *Cellulose* **27**, 4871–4887 (2020).
39. El-Naggar, M. E. et al. Potential antimicrobial and antibiofilm efficacy of essential oil nanoemulsion loaded polycaprolactone nanofibrous dermal patches. *Eur. Polymer J.* **184**, 111782 (2023).
40. Permanasari, A. E., Rambli, D. R. A. & Dominic, P. D. D. *Forecasting method selection using ANOVA and Duncan multiple range tests on time series dataset*. in *2010 International Symposium on Information Technology*. IEEE. (2010).
41. Cacciatore, F. A. et al. Carvacrol encapsulation into nanoparticles produced from Chia and flaxseed mucilage: characterization, stability and antimicrobial activity against *Salmonella* and *Listeria monocytogenes*. *Food Microbiol.* **108**, 104116 (2022).
42. Charles-Rodríguez, A. V. et al. Edible films based on black Chia (*Salvia hispanica* L.) seed mucilage containing *Rhus microphylla* fruit phenolic extract. *Coatings* **10** (4), 326 (2020).
43. Baji, A. et al. Electrospinning of Polymer nanofibers: effects on oriented morphology, structures and tensile properties. *Compos. Sci. Technol.* **70** (5), 703–718 (2010).
44. Ahmadian, A. et al. Overview of nano-fiber mats fabrication via electrospinning and morphology analysis. *Textiles* **1** (2), 206–226 (2021).
45. Matysiak, W. & Tański, T. Analysis of the morphology, structure and optical properties of 1D SiO<sub>2</sub> nanostructures obtained with sol-gel and electrospinning methods. *Appl. Surf. Sci.* **489**, 34–43 (2019).



46. Kim, S. et al. Nanofiber-based hydrocolloid from colloid electrospinning toward next generation wound dressing. *Macromol. Mater. Eng.* **301** (7), 818–826 (2016).
47. Karchoubi, F. et al. New insights into nanocomposite hydrogels; a review on recent advances in characteristics and applications. *Adv. Industrial Eng. Polym. Res.* **7** (1), 54–78 (2024).
48. Razavi, S. et al. Microencapsulating polymers for probiotics delivery systems: Preparation, characterization, and applications. *Food Hydrocoll.* **120**, 106882 (2021).
49. Zhu, Y. et al. Biomaterial-based encapsulated probiotics for biomedical applications: current status and future perspectives. *Mater. Design.* **210**, 110018 (2021).
50. Kim, H. J. et al. A comprehensive review of Li-ion battery materials and their recycling techniques. *Electronics* **9** (7), 1161 (2020).
51. Delattre, C. et al. Fabrication methods of sustainable hydrogels. In *Sustainable Polymer Composites and Nanocomposites* (eds. Inamuddin, Thomas, S., Kumar Mishra, R., Asiri, A.M.) 355–386 (Cham: Springer, 2019).
52. Maddela, N. R. et al. Functional determinants of extracellular polymeric substances in membrane biofouling: experimental evidence from pure-cultured sludge bacteria. *Appl. Environ. Microbiol.* **84** (15), e00756–e00718 (2018).
53. Orhan-Yanikan, E., Gülseren, G. & Ayhan, K. Protein profile of bacterial extracellular polymeric substance by Fourier transform infrared spectroscopy. *Microchem. J.* **156**, 104831 (2020).
54. Yin, C., Meng, F. & Chen, G. H. Spectroscopic characterization of extracellular polymeric substances from a mixed culture dominated by ammonia-oxidizing bacteria. *Water Res.* **68**, 740–749 (2015).
55. Hernández-Pérez, T. et al. *Chia (Salvia hispanica): nutraceutical properties and therapeutic applications*. in *Proceedings*. MDPI. (2020).
56. Zettel, V. & Hitzmann, B. Applications of Chia (*Salvia hispanica* L.) in food products. *Trends Food Sci. Technol.* **80**, 43–50 (2018).
57. Salgado, V. S. C. N. et al. *Chemical Composition, Fatty acid Profile, Phenolic Compounds, and Antioxidant Activity of raw and Germinated Chia (Salvia hispanica L.) Seeds* 78p. 735–741 (Plant Foods for Human Nutrition, 2023). 4.
58. Kassem, I. A. et al. *Mucilage as a Functional food Hydrocolloid: Ongoing and Potential Applications in Prebiotics and Nutraceuticals* 12p. 4738–4748 (Food & function, 2021). 11.
59. Souza, G. et al. Antioxidant activity, extraction and application of psyllium mucilage in chocolate drink. *Nutr. Food Sci.* **50** (6), 1175–1185 (2020).
60. Keshani-Dokht, S. et al. Extraction, chemical composition, rheological behavior, antioxidant activity and functional properties of *Cordia myxa* mucilage. *Int. J. Biol. Macromol.* **118**, 485–493 (2018).
61. Cuomo, F. et al. Effect of additives on Chia mucilage suspensions: a rheological approach. *Food Hydrocoll.* **109**, 106118 (2020).
62. Mujtaba, M. et al. Production of novel Chia-mucilage nanocomposite films with starch nanocrystals; an inclusive biological and physicochemical perspective. *Int. J. Biol. Macromol.* **133**, 663–673 (2019).
63. Lad, A., Rodge, P. & Khandelwal, K. Formulation Development of Antimicrobial Gel using Chia seed mucilage. *J. Pharm. Sci. Res.* **12** (12), 1489–1495 (2020).
64. Padil, V. V. T., Senan, C. & Černík, M. *Green polymeric electrospun fibers based on tree-gum hydrocolloids: fabrication, characterization and applications*, in *Materials for Biomedical Engineering*. Elsevier. pp. 127–172. (2019).
65. Srivastava, N. & Choudhury, A. R. *Enhanced encapsulation efficiency and controlled release of co-encapsulated Bacillus coagulans spores and vitamin B9 in gellan /κ-carrageenan/chitosan tri-composite hydrogel*. International Journal of Biological Macromolecules, 227: pp. 231–240. (2023).
66. Nezamdoost-Sani, N. et al. Alginate and derivatives hydrogels in encapsulation of probiotic bacteria: an updated review. *Food Bioscience.* **52**, 102433 (2023).
67. Ali, M. et al. Application of polysaccharides for the encapsulation of beneficial microorganisms for agricultural purposes: a review. *Int. J. Biol. Macromol.* **244**, 125366 (2023).
68. Nezamdoost-Sani, N. et al. A comprehensive review on the utilization of biopolymer hydrogels to encapsulate and protect probiotics in foods. *Int. J. Biol. Macromol.* **254**, 127907 (2024).
69. Shekarfroush, E. et al. Electrospun phospholipid fibers as micro-encapsulation and antioxidant matrices. *Molecules* **22** (10), 1708 (2017).
70. Nawaz, A. et al. Fabrication and characterization of Apple-Pectin-PVA-Based nanofibers for Improved viability of Probiotics. *Foods* **12** (17), 3194 (2023).
71. Ma, J. et al. Enhanced viability of probiotics encapsulated within synthetic/natural biopolymers by the addition of gum arabic via electrohydrodynamic processing. *Food Chem.* **413**, 135680 (2023).
72. Simonić, M. et al. Probiotic *Lactobacillus paracasei* K7 nanofiber encapsulation using nozzle-free electrospinning. *Appl. Biochem. Biotechnol.* **195** (11), 6768–6789 (2023).
73. Vaishnavi, S. & Preetha, R. *Soy protein incorporated nanoemulsion for enhanced stability of probiotic (Lactobacillus delbrueckii subsp. bulgaricus) and its characterization*. Materials Today: Proceedings, 40: pp. S148–S153. (2021).
74. Barradas, T. N. & de Silva, K. G. *Nanoemulsions of essential oils to improve solubility, stability and permeability: a review*. Environmental Chemistry Letters, 19(2): pp. 1153–1171. (2021).
75. Zare, M. & Ramakrishna, S. *Current progress of electrospun nanocarriers for drug delivery applications*. in *Proceedings*. (2020).
76. Thongchaivetcharat, K., Jenjob, R. & Crespy, D. Encapsulation and release of functional nanodroplets entrapped in nanofibers. *Small* **14** (20), 1704527 (2018).
77. Mickova, A. et al. Core/shell nanofibers with embedded liposomes as a drug delivery system. *Biomacromolecules* **13** (4), 952–962 (2012).
78. Dehcheshmeh, M. A. & Fathi, M. Production of core-shell nanofibers from zein and tragacanth for encapsulation of saffron extract. *Int. J. Biol. Macromol.* **122**, 272–279 (2019).
79. Madybekova, G. et al. Study of probiotic Bacteria encapsulation for potential application in Enrichment of Fermented Beverage. *Colloids Interfaces.* **8** (5), 51 (2024).
80. Krithika, B. & Preetha, R. Formulation of protein based inulin incorporated synbiotic nanoemulsion for enhanced stability of probiotic. *Mater. Res. Express.* **6** (11), 114003 (2019).
81. Alizadeh, A. M. et al. Electrospun fibers loaded with probiotics: fundamentals, characterization, and applications. *Probiotics Antimicrob. Proteins.* **16** (3), 1099–1116 (2024).

## Author contributions

Shirin Rashnoei: Investigation, Writing- Original draft preparation. Mozghan Shahamirian and Sedigheh Yazdanpanah: Investigation, Supervision, Resources, Writing- Reviewing and Editing. Elham Ansarifard: Reviewing and Editing.

## Funding

This research did not receive any specific grant from funding agencies.



## Declarations

### Competing interests

The authors declare that they have no known competing financial interests or personal relationships that could have appeared to influence the work reported in this paper.

### Additional information

**Correspondence** and requests for materials should be addressed to M.S.

**Reprints and permissions information** is available at [www.nature.com/reprints](http://www.nature.com/reprints).

**Publisher's note** Springer Nature remains neutral with regard to jurisdictional claims in published maps and institutional affiliations.

**Open Access** This article is licensed under a Creative Commons Attribution-NonCommercial-NoDerivatives 4.0 International License, which permits any non-commercial use, sharing, distribution and reproduction in any medium or format, as long as you give appropriate credit to the original author(s) and the source, provide a link to the Creative Commons licence, and indicate if you modified the licensed material. You do not have permission under this licence to share adapted material derived from this article or parts of it. The images or other third party material in this article are included in the article's Creative Commons licence, unless indicated otherwise in a credit line to the material. If material is not included in the article's Creative Commons licence and your intended use is not permitted by statutory regulation or exceeds the permitted use, you will need to obtain permission directly from the copyright holder. To view a copy of this licence, visit <http://creativecommons.org/licenses/by-nc-nd/4.0/>.

© The Author(s) 2025